Supplementary Figure 1

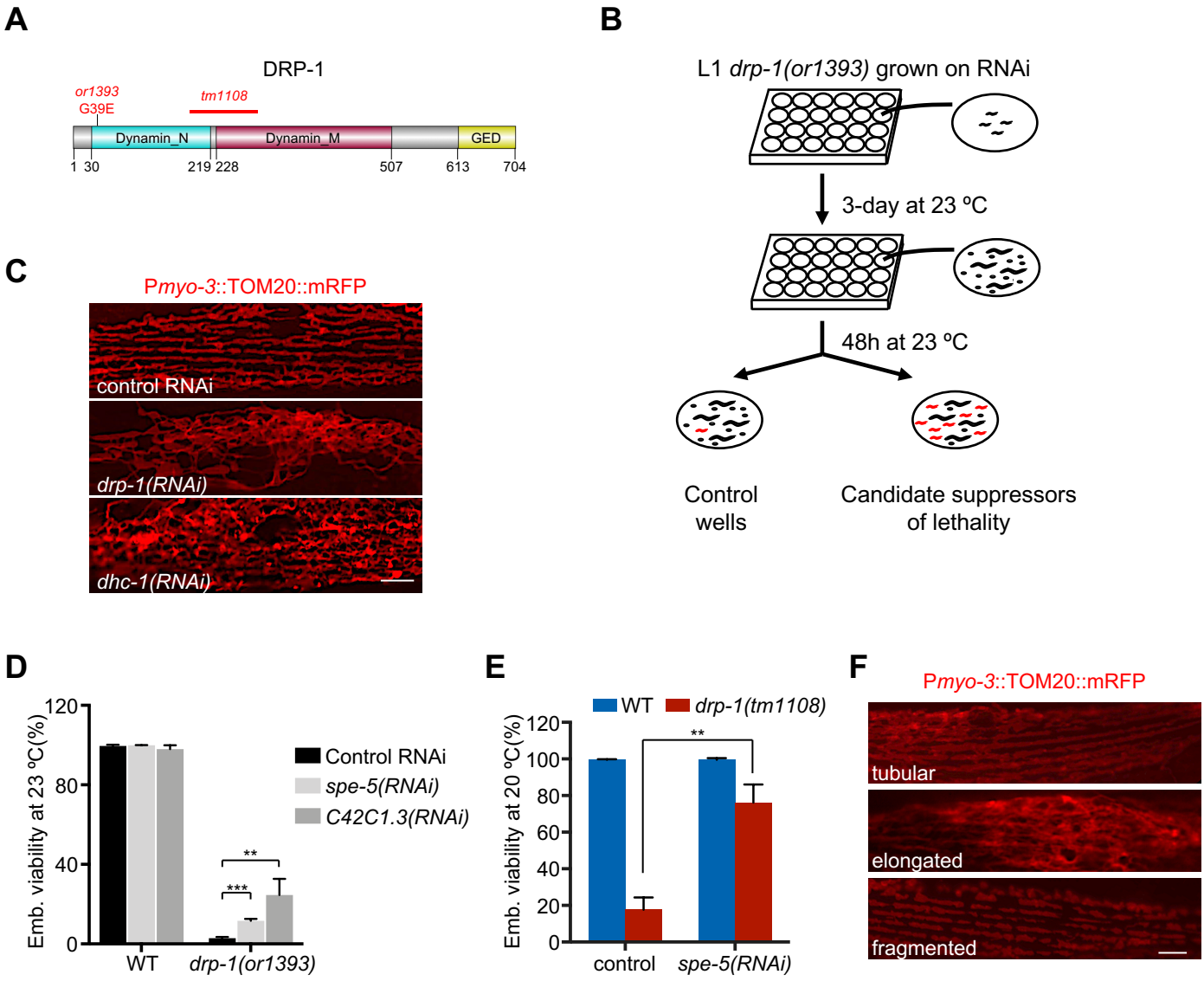

Fig. S1. RNAi screen identifies gene inactivation suppresses *drp-1* lethality

(*A*) Schematic of the DRP-1 protein and the *drp-1(or1393)* and *drp-1(tm1108)* mutations.

(*B*) Diagram of the RNAi screen workflow for suppressors of *drp-1(or1393)* lethality. See Methods for details.

(*C*) Mitochondrial morphology in body wall muscles after indicated RNAi treatment. Scale bar, 5 μm.

(*D*) Viability of wild-type and *drp-1(or1393)* after indicated RNAi treatment at 23°C. Mean ± s.d. ***$P < 0.001$, **$P < 0.01$.

(*E*) Viability of wild-type and *drp-1(tm1108)* in control versus *spe-5(RNAi)* animals. Mean ± s.d. **$P < 0.01$.

(*F*) Examples of tubular, elongated and fragmented mitochondria in body wall muscles in wild-type. Scale bar, 5 μm.

Supplementary Figure 2

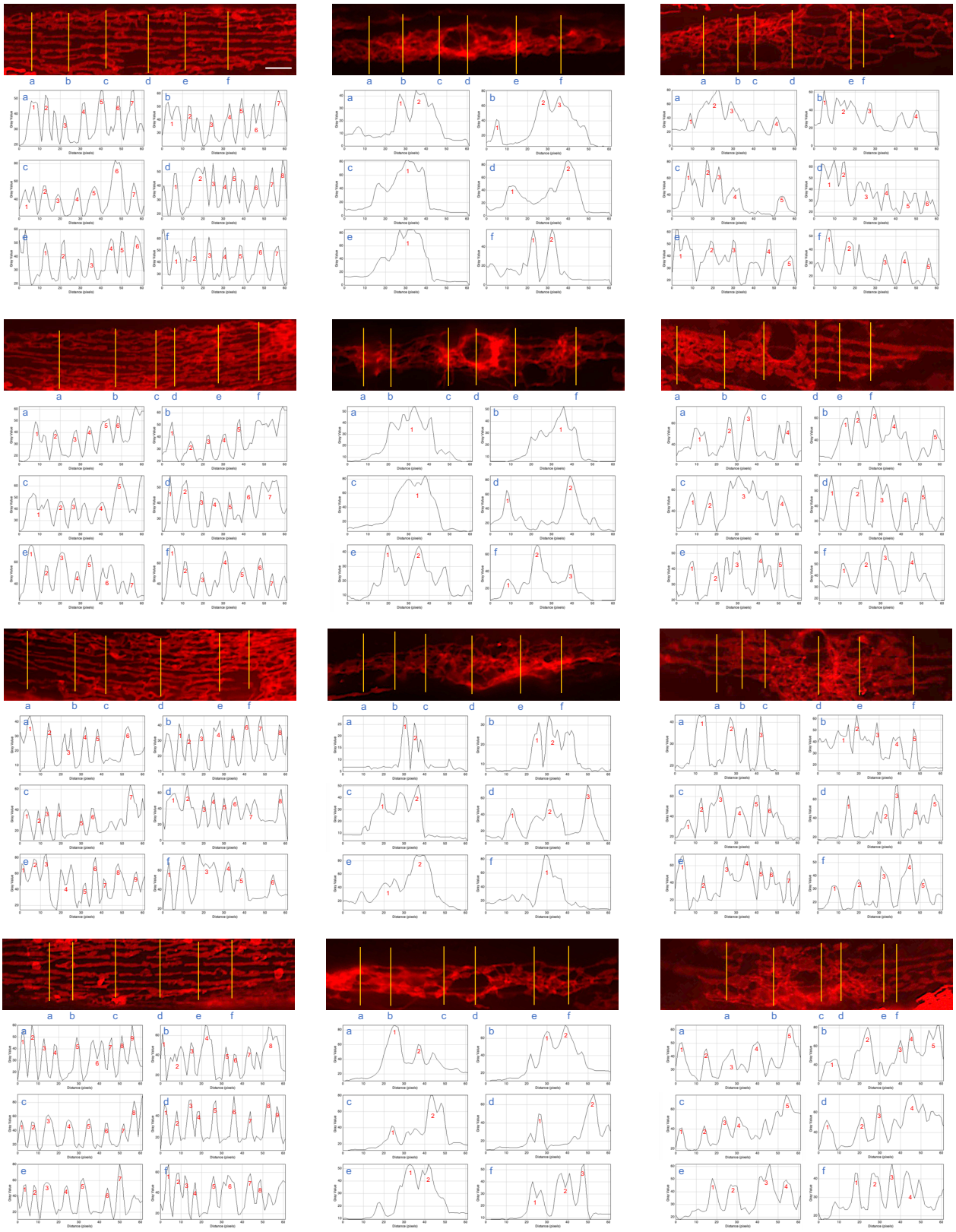

Fig. S2. Representative images of mitochondrial morphology in indicated animals

Mitochondrial morphology of wild-type and *drp-1(tm1108)* in control versus *spe-5(RNAi)* in a single body wall muscle cell. Mitochondria are visualized by a mitochondrial outer membrane localized mRFP fusion protein. Lower panels are plot profiles of the cross sections indicated by yellow lines. Criterion for a peak: peak to trough (both sides) > 20 Grey value units (y units). Scale bar, 5 μm.

Supplementary Figure 3

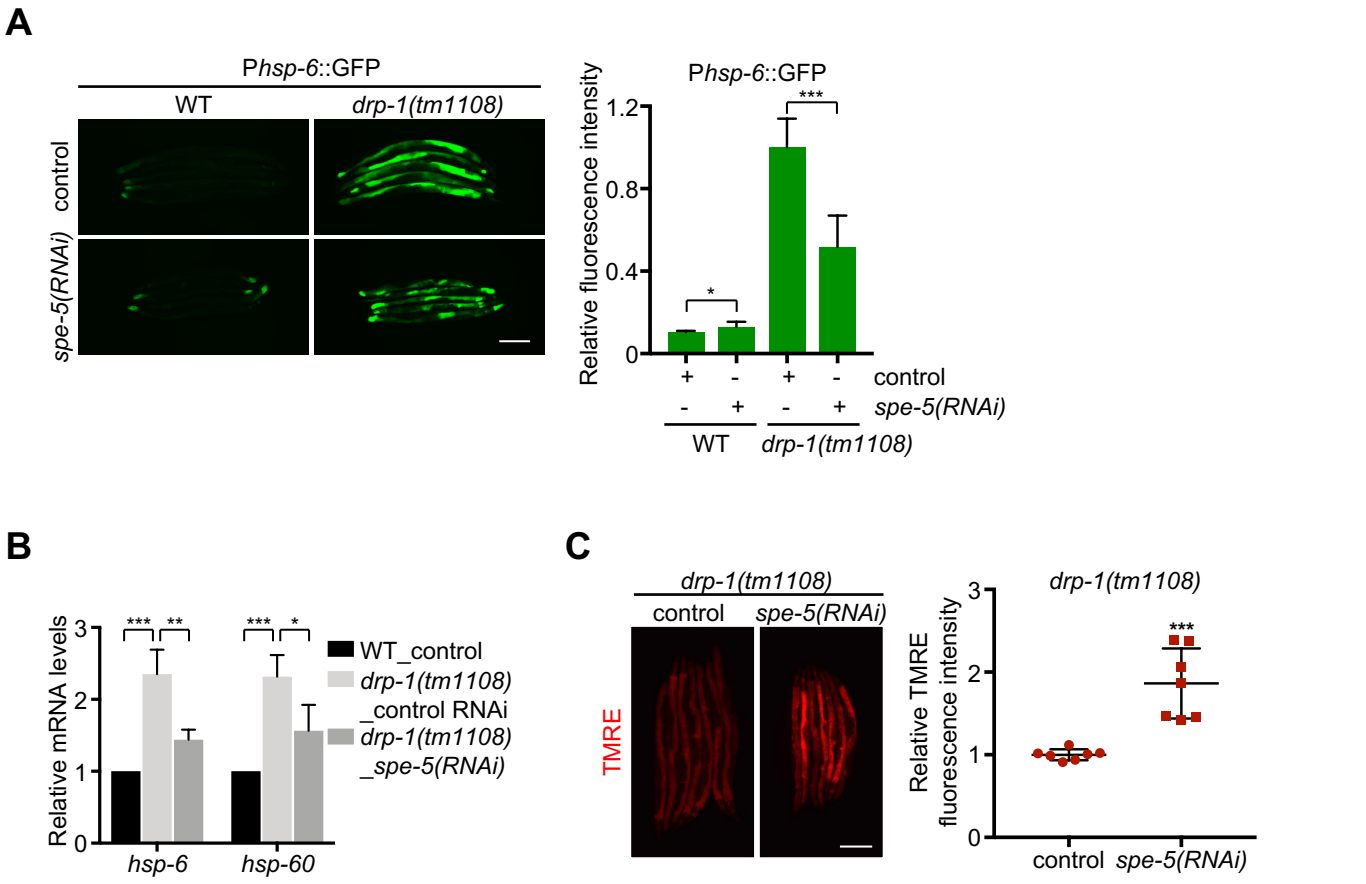

Fig. S3. Inactivation of the vacuolar ATPase *spe-5* suppresses *drp-1* mitochondrial defects

(*A*) P*hsp-6*::GFP expression in wild-type and *drp-1(tm1108)* animals grown on control versus *spe-5(RNAi)*. Mean ± s.d. ***$P < 0.001$, *$P < 0.05$. Scale bar, 0.2 mm.

(*B*) Endogenous expression levels of mitochondrial chaperone genes *hsp-6* and *hsp-60* in indicated animals. Mean ± s.d. from at least three biological replicates. ***$P < 0.001$, **$P < 0.01$, *$P < 0.05$.

(*C*) Animals with indicated treatment were stained with TMRE (tetramethylrhodamine, ethyl ester). Mean ± s.d. ***$P <$ 0.001. Scale bar, 0.2 mm.

Supplementary Figure 4

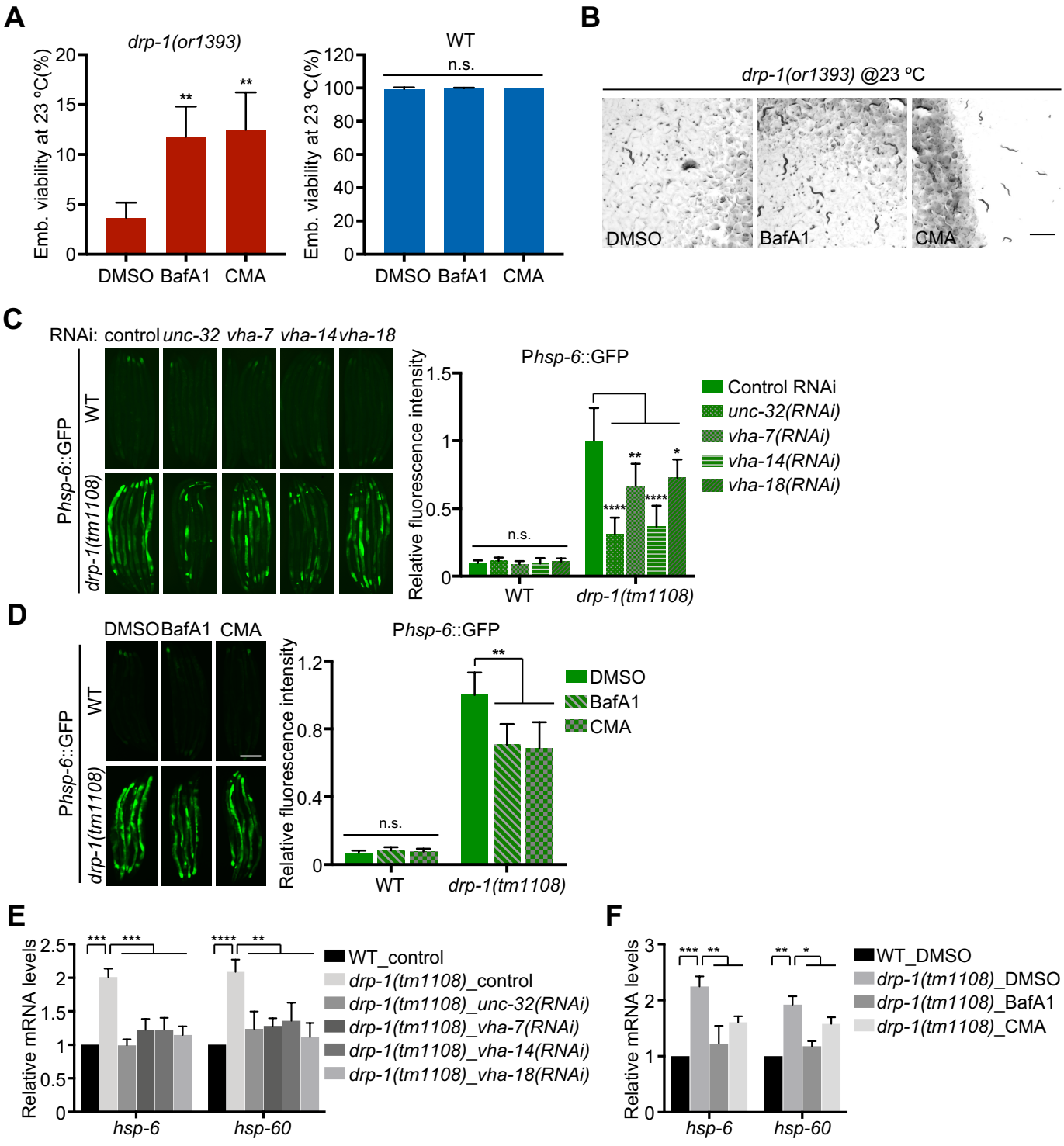

Fig. S4. Disruptions of V-ATPase activity suppress *drp-1* lethality and mitochondrial defects

(*A*, *B*) Viability of wild-type and *drp-1(or1393)* with DMSO, BafA1 or CMA treatment at 23°C. DMSO, solvent control; BafA1, bafilomycin A1; CMA, concanamycin A. Mean ± s.d. $^{**}P < 0.01$. Scale bar, 1 mm.

(*C*, *D*) P*hsp-6*::GFP expression in wild-type and *drp-1(tm1108)* animals with indicated treatment. Mean ± s.d. $^{****}P < 0.0001$, $^{**}P < 0.01$, $^{*}P < 0.05$. n.s., not significant. Scale bar, 0.2 mm.

(*E*, *F*) Endogenous expression levels of mitochondrial chaperone genes *hsp-6* and *hsp-60* in animals with indicated treatment. Mean ± s.d. from at least three biological replicates. $^{****}P < 0.0001$, $^{***}P < 0.001$, $^{**}P < 0.01$, $^{*}P < 0.05$.

Supplementary Figure 5

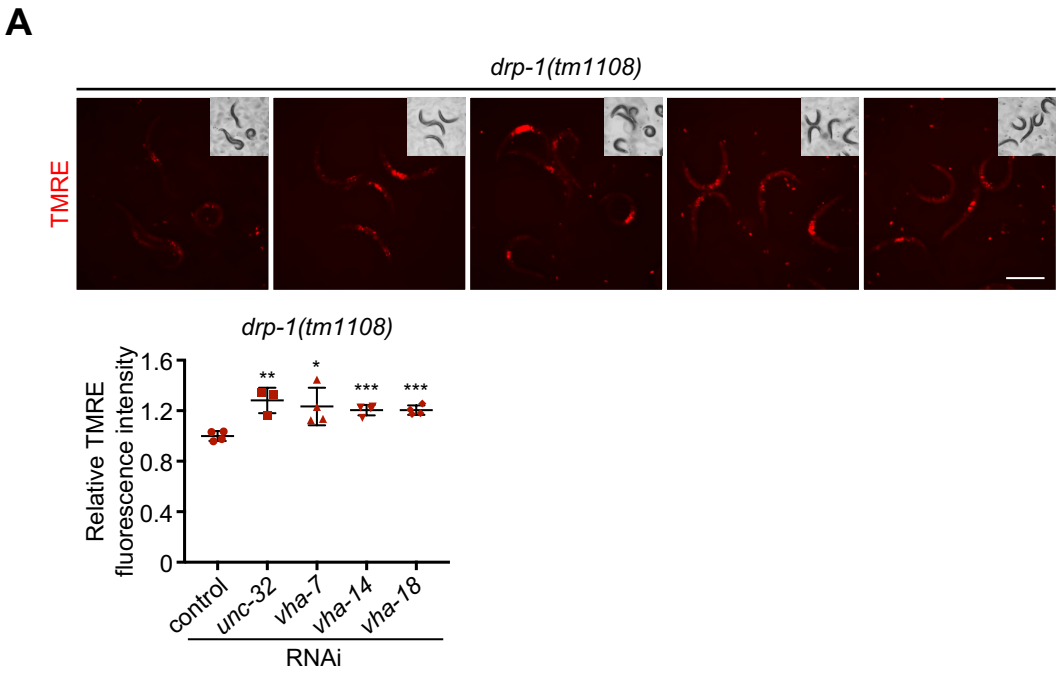

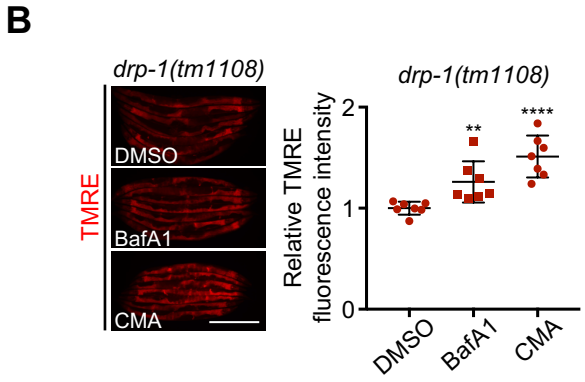

Fig. S5. Inhibitions of V-ATPase activity increase mitochondrial membrane potential in *drp-1(tm1108)*

(*A*, *B*) Animals with indicated treatment were stained with TMRE. Mean ± s.d. ****$P < 0.0001$, **$P < 0.01$. Scale bar, 0.4 mm.

Supplementary Figure 6

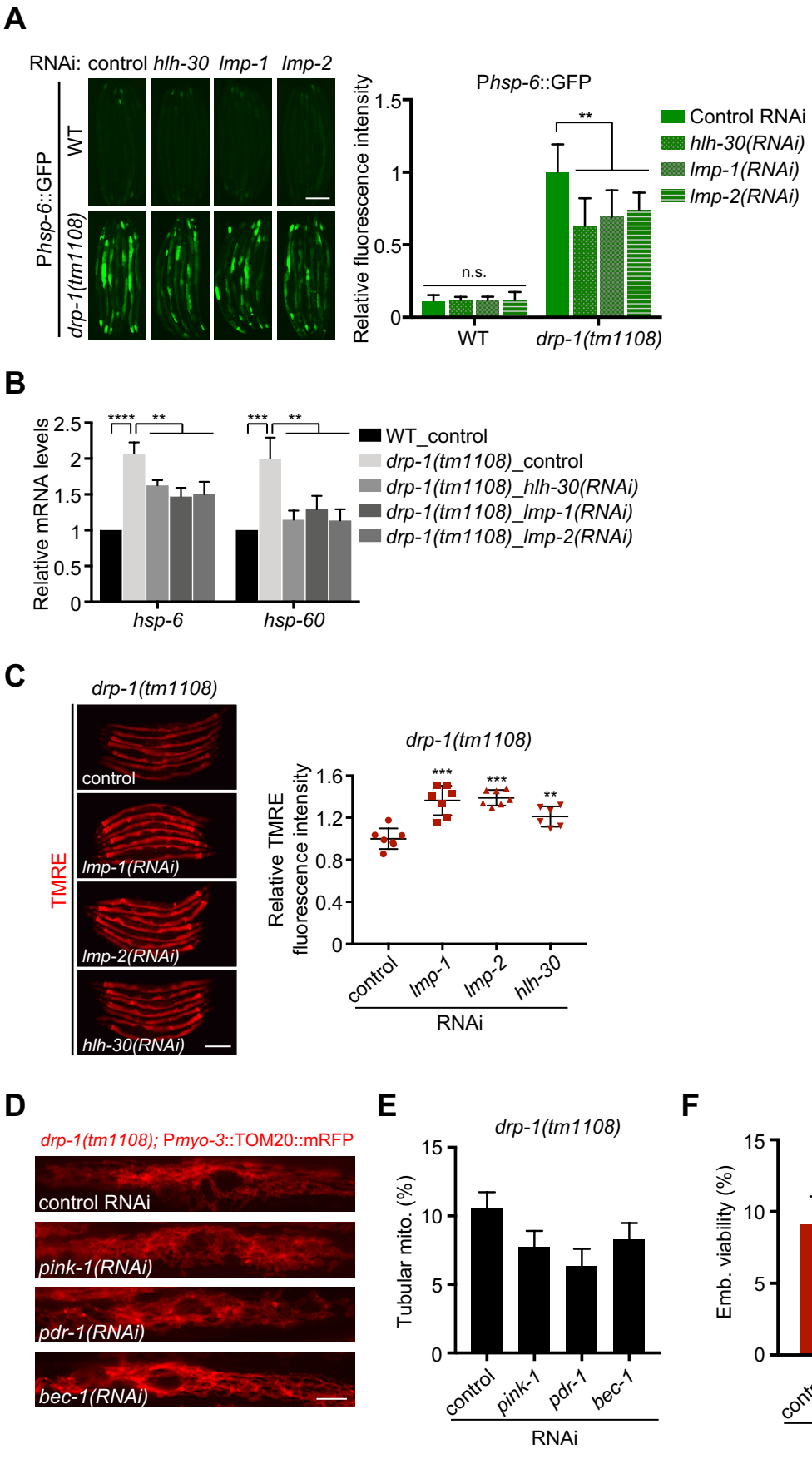

Fig. S6. Lysosomal dysfunction suppresses *drp-1* mitochondrial fission defects

(*A*) P*hsp-6*::GFP expression in wild-type and *drp-1(tm1108)* animals grown on control or indicated RNAi bacteria clones. Mean ± s.d. $^{**}P < 0.01$. n.s., not significant. Scale bar, 0.2 mm.

(*B*) Endogenous expression levels of mitochondrial chaperone genes *hsp-6* and *hsp-60* in animals with indicated treatment. Mean ± s.d. from at least three biological replicates. $^{****}P < 0.0001$, $^{***}P < 0.001$, $^{**}P < 0.01$.

(*C*) Animals with indicated treatment were stained with TMRE. Mean ± s.d. $^{***}P < 0.001$, $^{**}P < 0.01$. Scale bar, 0.2 mm.

(*D*) Mitochondrial morphology in *drp-1(tm1108)* body wall muscles after indicated RNAi treatment. Scale bar, 5 μm.

(*E*) Percentage of mitochondria with tubular morphology in *drp-1(tm1108)* body wall muscles after indicated RNAi treatments. Mean ± s.d.

(*F*) Viability of *drp-1(or1393)* after mitophagy gene inactivations at 23°C.

Supplementary Figure 7

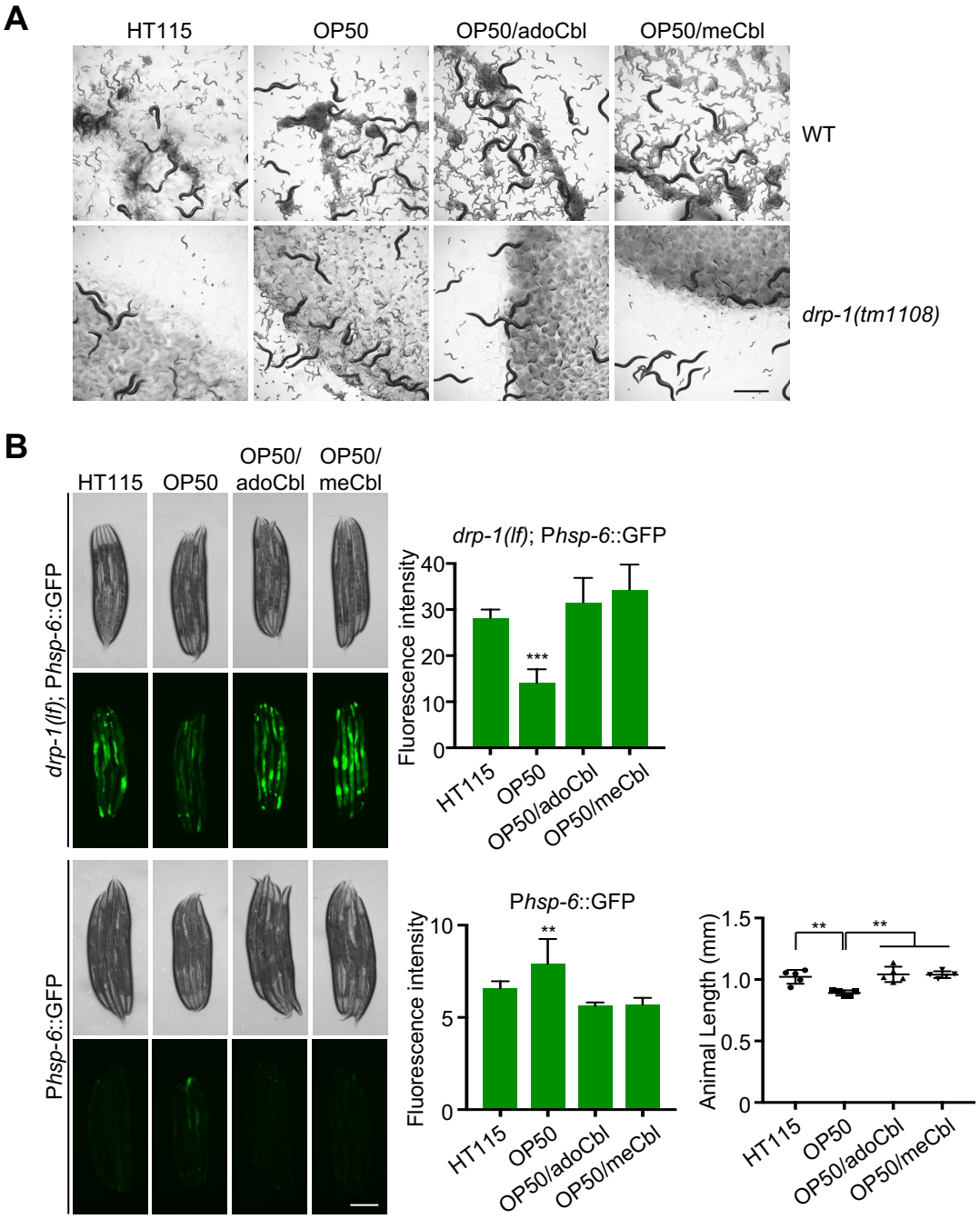

Fig. S7. Dietary B12 deficiency suppresses *drp-1* defects

(*A*) Growth of wild-type (WT) and *drp-1(tm1108)* fed on *E. coli* HT115 or *E. coli* OP50 with or without B12 supplementation at 20°C for 5-day since embryos. Scale bar, 1 mm.

(*B*) P*hsp-6*::GFP expression and animal lengths in wild-type and *drp-1(lf)* animals raised on *E. coli* HT115 or *E. coli* OP50 with or without B12 supplementation. Mean ± s.d. ***$P < 0.001$, **$P < 0.01$. *drp-1(lf)*, *drp-1(tm1108)*. Scale bar, 0.2 mm.

Supplementary Figure 8

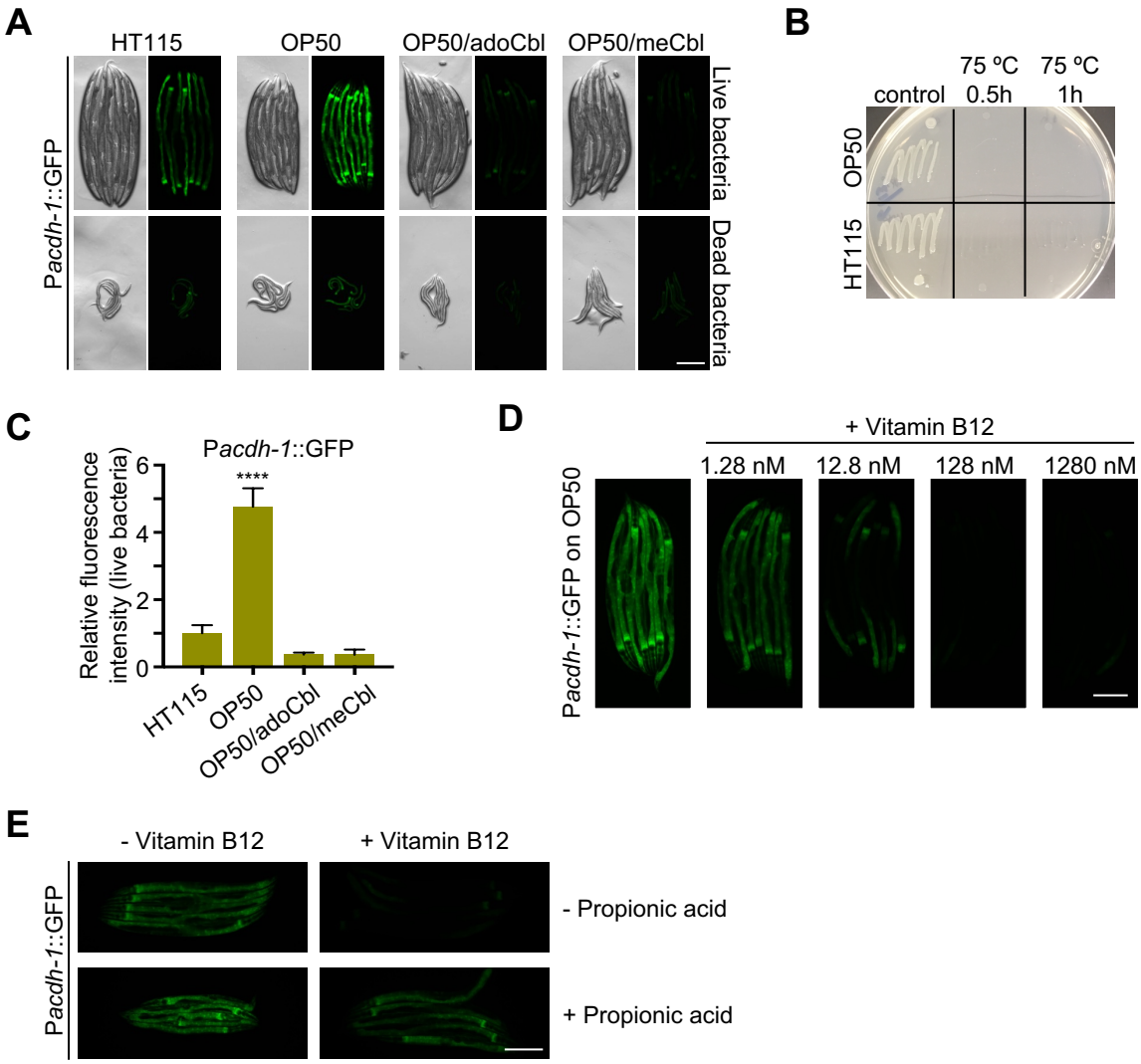

Fig. S8. P*acdh-1*::GFP as vitamin B12 indicator

(*A*) P*acdh-1*::GFP animals raised on live (upper panels) or dead (75°C 0.5h, lower panels) *E. coli* HT115 or *E. coli* OP50 with or without B12 supplementation. Scale bar, 0.2 mm.

It is possible that *E. coli* K12 and *E. coli* B strains metabolize B12 differently to affect the animals grown on them. To exclude this possibility, we killed the *E. coli* bacteria by heat. Incubation of the *E. coli* bacteria at 70°C for 30 min was enough to completely kill them. Animals fed on dead bacteria induced P*acdh-1*::GFP on *E. coli* OP50 (B12 deficient) diets, although much milder than those fed on live bacteria.

(*B*) Bacteria with or without heat treatment grown on LB agar plate at 37°C overnight.

(*C*) P*acdh-1*::GFP expression for animals raised on live *E. coli* HT115 or *E. coli* OP50 with or without B12 supplementation. Mean ± s.d. ****$P < 0.0001$.

(*D*) P*acdh-1*::GFP expression for animals raised on *E. coli* OP50 without or with different doses of vitamin B12 supplementation. Scale bar, 0.2 mm.

(*E*) P*acdh-1*::GFP expression for animals raised on *E. coli* OP50 with or without propionic acid treatment and B12 supplementation. Propionic acid treatment induced P*acdh-1*::GFP, which was suppressed by vitamin B12 supplementation. Scale bar, 0.2 mm.

Supplementary Figure 9

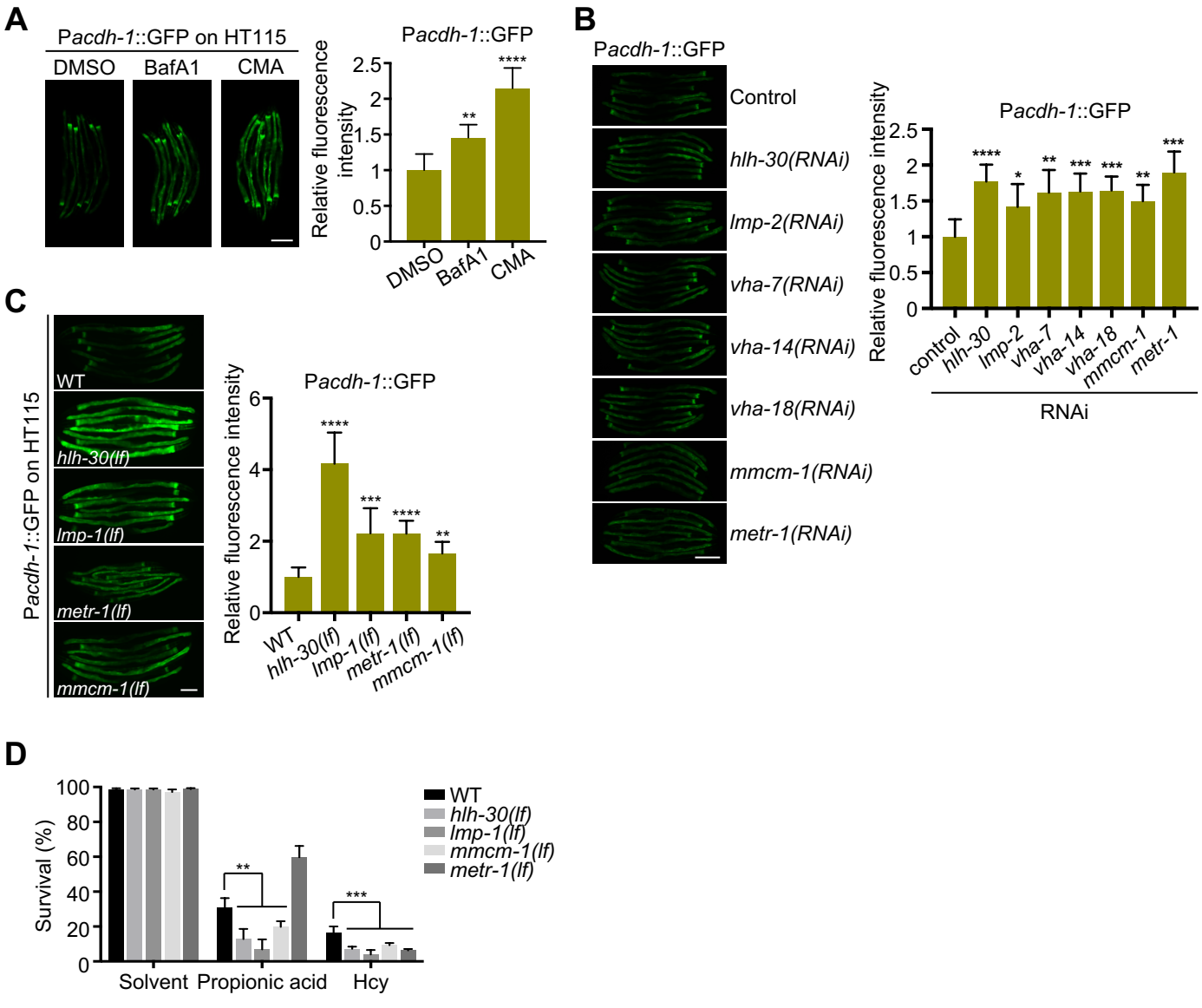

Fig. S9. Lysosomal dysfunction leads to B12 deficiency

(*A*, *B*) P*acdh-1*::GFP expression for animals with indicated treatment. Mean ± s.d. ****$P < 0.0001$, ***$P < 0.001$, **$P < 0.01$, *$P < 0.05$. Scale bar, 0.2 mm.

(*C*) P*acdh-1*::GFP expression for animals with indicated genetic mutation background. Mean ± s.d. ****$P < 0.0001$, ***$P < 0.001$, **$P < 0.01$. Scale bar, 0.1 mm.

(*D*) Survival of animals treated with solvent control, 100 mM propionic acid, or 15 mM homocysteine (Hcy). Mean ± s.d. ***$P < 0.001$, **$P < 0.01$.

Although the propionate shunt is activated when the cellular B12 level is low to breakdown the excess propionate, high propionate loading saturates the propionate shunt. Indeed, a *C. elegans mmcm-1* loss-of-function mutation reduced the survival of animals in the presence of 100 mM propionic acid, consistent with the finding that deletion of PCCA-1, an upstream enzyme of the canonical propionate breakdown pathway, reduced the LD_{50} for propionate (1). The *metr-1* methionine synthetase loss-of-function mutation caused animals to be resistant to a high concentration of propionate on an *E. coli* OP50 diet, similar to previous observation (2). Deletion of either *mmcm-1* or *metr-1* caused animals to become hypersensitive to exogenously supplementation of 15 mM homocysteine. Both *hlh-30(lf)* and *lmp-1(lf)* lysosomal mutants were hypersensitive to 100 mM propionic acid and 15 mM homocysteine compared to wild-type, suggesting B12 deficiency in these lysosomal mutants. Overall, these findings indicate that lysosomal dysfunction causes B12 deficiency in animals that were fed B12 proficient *E. coli* HT115 K12 strains, which usually provide enough vitamin B12 to wild-type animals.

Supplementary Figure 10

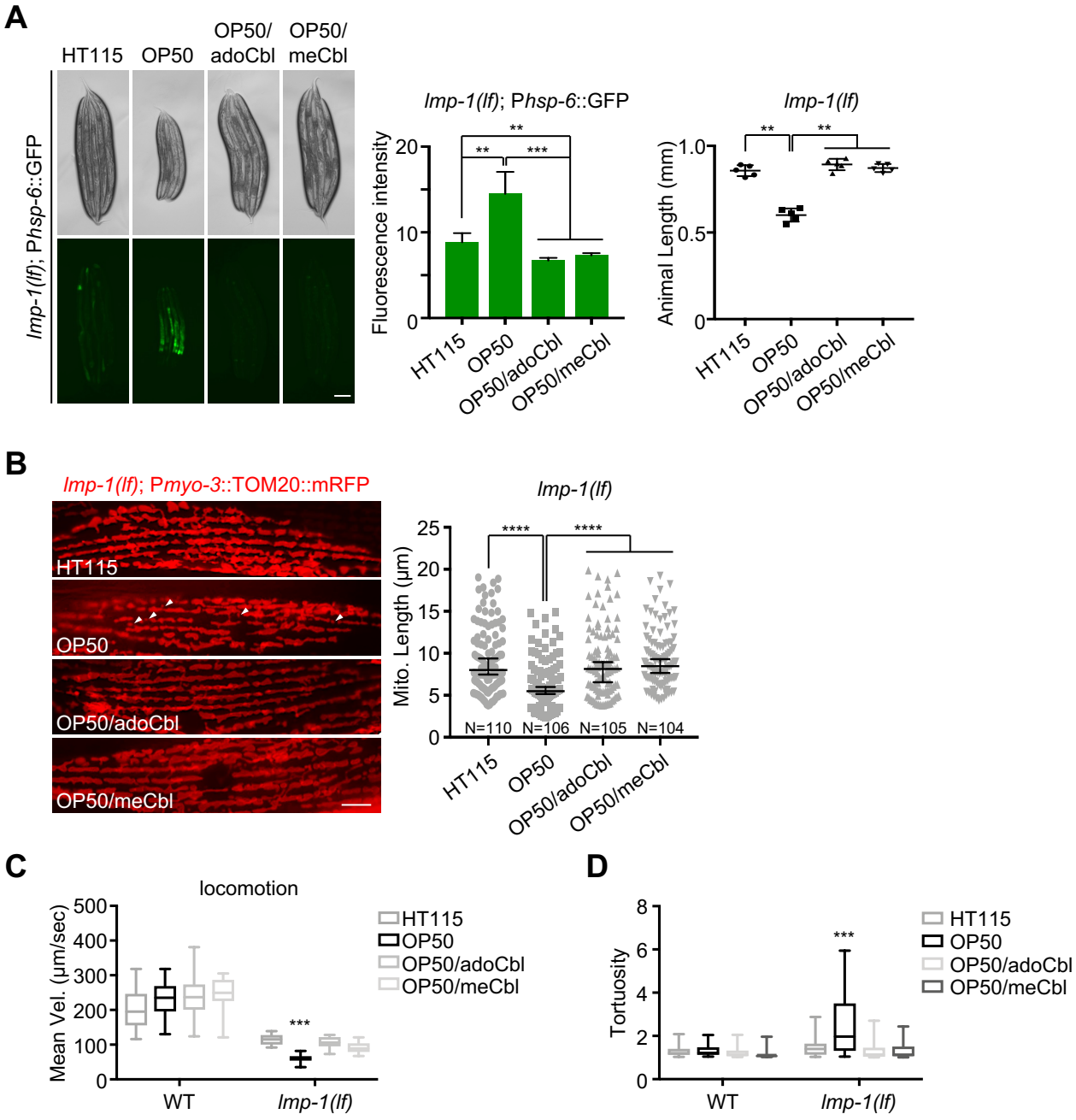

Fig. S10. Dietary B12 supplementation rescues mitochondrial fragmentation and locomotion defects caused by lysosomal dysfunction

(*A*) *lmp-1(lf)*; P*hsp-6*::GFP animals fed on *E. coli* HT115 or *E. coli* OP50 with or without B12 supplementation. Mean ± s.d. ***$P < 0.001$, **$P < 0.01$. Scale bar, 0.1 mm.

(*B*) Mitochondrial morphologies and lengths in body wall muscles in *lmp-1(lf)* fed on *E. coli* HT115 or *E. coli* OP50 with or without B12 supplementation. Arrows mark some examples of fragmented mitochondria. Mitochondrial lengths were calculated by MiNA toolset. Median with 95% C. I. Mann-Whitney test. ****$P < 0.0001$. N indicates the sample size. Scale bar, 5 μm.

(*C*, *D*) Locomotion movement of wild-type (WT) or *lmp-1(lf)* fed on *E. coli* HT115 or *E. coli* OP50 with or without B12 supplementation. n=25~40. ***$P < 0.001$.

Supplementary Figure 11

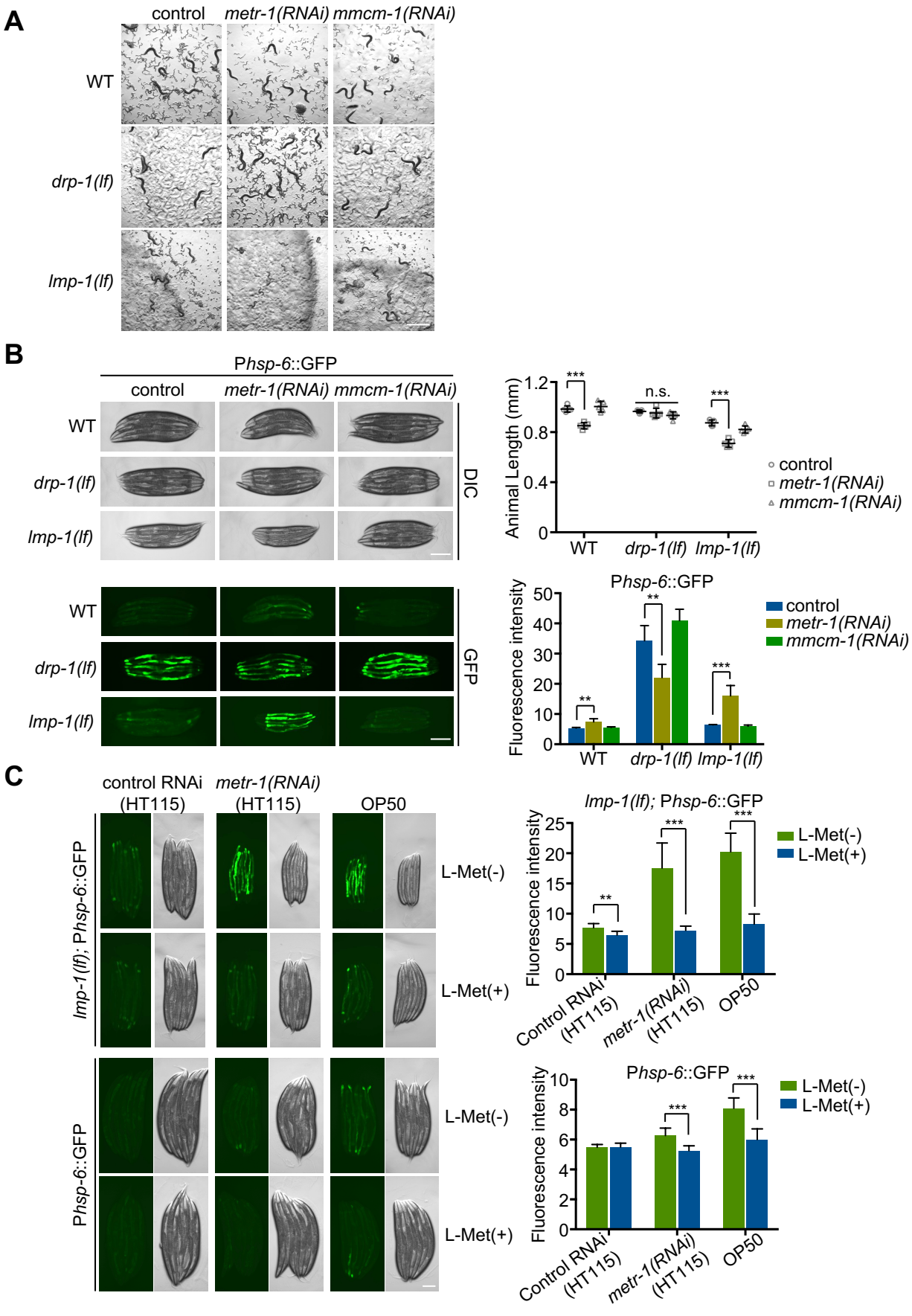

Fig. S11. Methionine restriction increases mitochondrial fission

(*A*) Development of wild-type, *lmp-1(lf)* or *drp-1(lf)* grown on indicated RNAi clones. Scale bar, 1 mm

(*B*) P*hsp-6*::GFP with wild-type, *lmp-1(lf)* and *drp-1(lf)* background animals grown on indicated RNAi clones. Mean ± s.d. ***$P < 0.001$, **$P < 0.01$. n.s., not significant. Scale bar, 0.2 mm.

(*C*) P*hsp-6*::GFP expression in *lmp-1(lf)* (upper panels) and wild-type (lower panels) animals grown on indicated bacteria with or without methionine supplementation. Mean ± s.d. ***$P < 0.001$, **$P < 0.01$. Scale bar, 0.1 mm.

Supplementary Figure 12

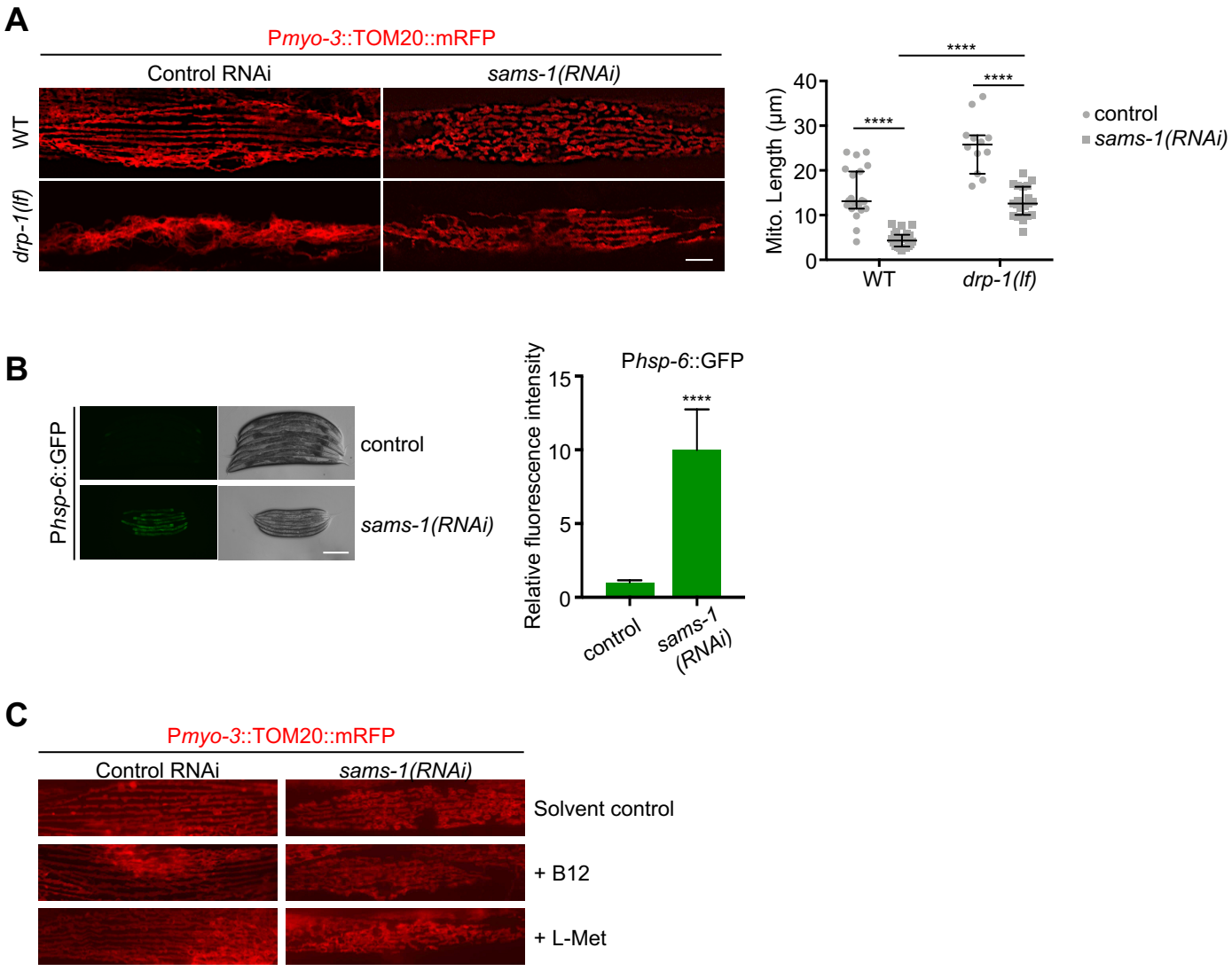

Fig. S12. Inactivation of *sams-1* increases mitochondrial fission

(*A*) Mitochondrial morphology in wild-type and *drp-1(lf)* body wall muscles after indicated RNAi treatment. Mitochondrial lengths were calculated by MiNA toolset. Median with 95% C. I. Mann-Whitney test. ****$P < 0.0001$. Scale bar, 5 μm.

(*B*) P*hsp-6*::GFP animals grown on control versus *sams-1(RNAi)*. Mean ± s.d. ****$P < 0.0001$. Scale bar, 0.2 mm.

(*C*) Mitochondrial morphology in animals grown on control or *sams-1(RNAi)* after indicated treatment. Scale bar, 5 μm.

Supplementary Figure 13

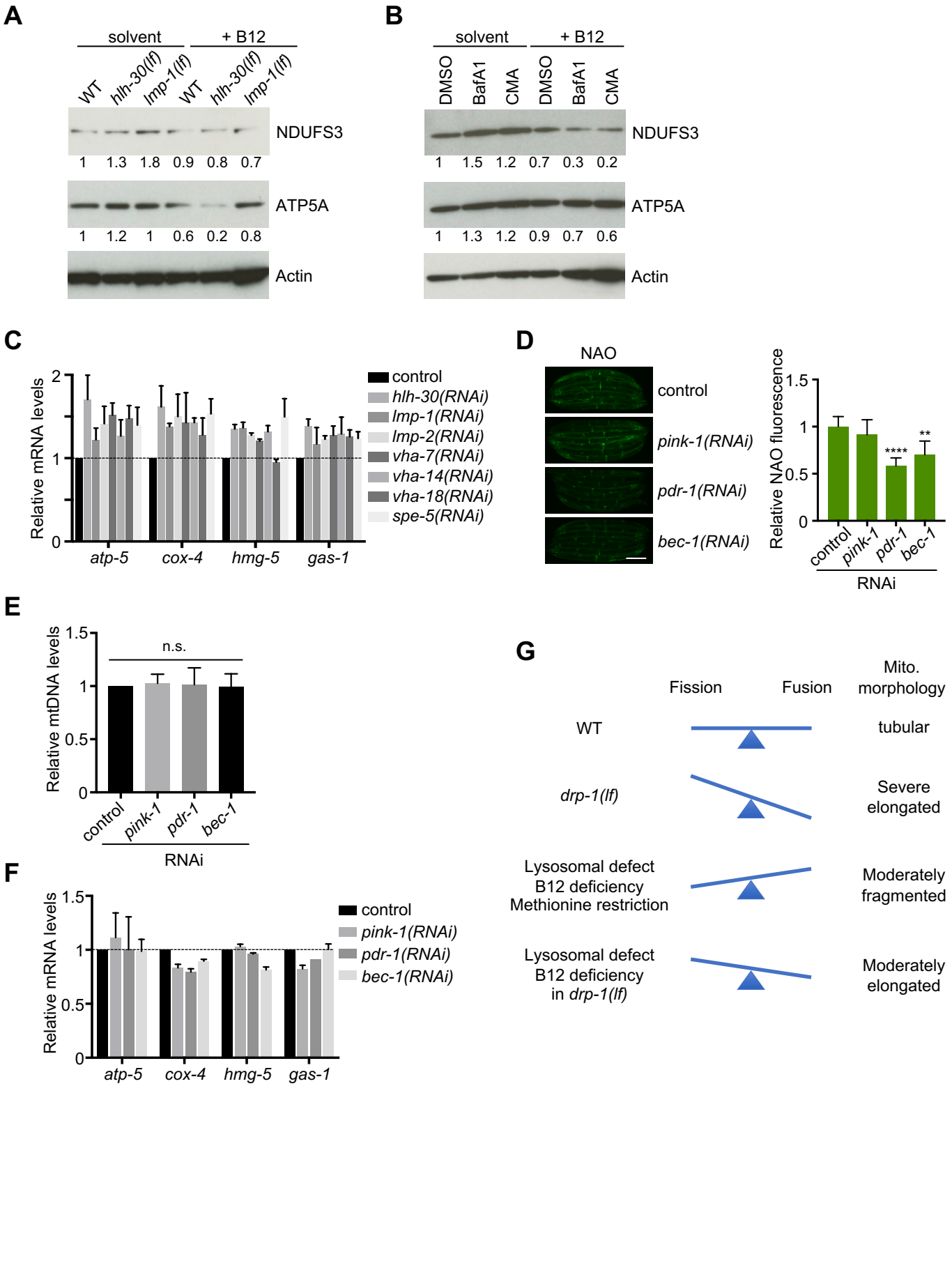

Fig. S13. Lysosomal dysfunction increases mitochondrial mass by inducing mitochondrial biogenesis

(*A*, *B*) Immunoblots of lysates from animals with indicated treatment. Relative protein levels were indicated below the gel lanes.

(*C*, *F*) Expression levels of mitochondrial biogenesis genes *atp-5*, *cox-4 hmg-5* and *gas-1* in animals after indicated RNAi treatment. Mean ± s.d. from at least three biological replicates.

(*D*) Animals with mitophagy gene inactivations were stained with Nonyl Acridine Orange (NAO). Mean ± s.d. ****$P < 0.0001$, **$P < 0.01$. Scale bar, 0.2 mm.

(*E*) Relative mitochondrial DNA levels in control and mitophagy defective animals. Mean ± s.d. from at least three biological replicates. n.s., not significant.

(*G*) The schematic diagram of the balance of mitochondrial fission-fusion events under different physiological condition.

REFERENCES

1. Watson E, et al. (2016) Metabolic network rewiring of propionate flux compensates vitamin B12 deficiency in C. elegans. *Elife* 5:2807.

2. Watson E, et al. (2014) Interspecies systems biology uncovers metabolites affecting C. elegans gene expression and life history traits. *Cell* 156(4):759–770.